

## Original Articles

# Multi-scenario simulation of land use/land cover change and water yield evaluation coupled with the GMOP-PLUS-InVEST model: A case study of the Nansi Lake Basin in China

Yingchun Liu <sup>a,b</sup>, Yande Jing <sup>a,b,\*</sup>, Shanmei Han <sup>a,b</sup><sup>a</sup> College of Geography and Tourism, Qufu Normal University, Rizhao 276826, China<sup>b</sup> Rizhao Key Laboratory of Land Spatial Planning and Ecological Construction, Rizhao 276826, China

## ARTICLE INFO

## ABSTRACT

## Keywords:

Multi-scenario simulation  
Water yield  
GMOP-PLUS-InVEST model  
Nansi Lake Basin

Changes in land use/land cover (LULC) can impact water yield (WY) by altering the structural layout and functions of terrestrial ecosystems. Therefore, to ensure regional economic and ecosystem sustainability, it is critical to investigate the correlation between LULC change and WY. The GMOP-PLUS-InVEST (GPI) coupling model based on the gray multi-objective optimization model, the patch-generating land use simulation model, and the integrated valuation of ecosystem services and trade-offs model was used in this study. Establishing three different scenarios: business as usual (BAU), economic development scenario (ED), and ecological conservation scenario (EC) to predict the LULC distribution pattern in the Nansi Lake Basin (NLB) in 2035, and obtain the WY from 2000 to 2035. Getis-Ord Gi\* and Anselin Local Moran's I were used to investigate the spatial-temporal features of WY at the grid scale. The results indicated that: (1) The dominant LULC types of the NLB were farmland and construction land. The primary transfer trend was construction land encroaching on farmland due to the acceleration of the urbanization process and policy intervention. (2) The results of the LULC simulation in the NLB in 2035 showed that the BAU had a continuous trend of change for nearly 20 years; Under the ED, the intensity of construction land encroachment on farmland was accelerating; Under the EC, an apparent increase in the proportion of ecological land could be seen, and the contradiction between construction land and farmland had eased, which was expected to be more in line with the policy and planning objectives. (3) LULC change had a significant effect on WY. From 2000 to 2035, WY of the NLB continued to increase, and in 2035, the WY under different scenarios was ED > EC > BAU. Spatially it always showed a high value distribution in the south and west in the NLB. The GPI coupling model can be used for LULC optimization and ecosystem service evaluation, providing ideas for rational planning of future LULC. Research results have significant reference significance for the formulation of LULC policies and the protection and restoration of ecological environment of the NLB.

## 1. Introduction

Water yield (WY) in ecosystem services is the foundation of various ecological processes and ecological service functions (Wang et al., 2022b), which is crucial to intercepting precipitation, regulating runoff, purifying water quality, improving hydrological conditions and regulating regional water circulation (Benra et al., 2021), and is related to human well-being in the basin (Wu et al., 2022). Since the 21st century, industrialization and urbanization had caused a series of problems in the land resource development and utilization, leading to the degradation of water ecological functions in basins, the decline in water ecosystem services, and the growing conflict between human

development and ecological conservation. The level of WY is a product of the combination of natural environment and human activities, among which land use/land cover (LULC) change directly and indirectly affects hydrological processes and water resource utilization, and is a critical driver for changes in WY in basins (Yang et al., 2021). Investigating the response of WY to future LULC changes has become a critical topic in contemporary geography and ecology research. In this context, research on LULC and WY is essential towards understanding how human activities impact regional WY and has significant implications for conducting regional ecological protection and formulating planning policies for sustainable development that balances ecological conservation and economic growth (Balist et al., 2022).

\* Corresponding author at: College of Geography and Tourism, Qufu Normal University, Rizhao 276826, China.

E-mail address: [jyd7785@qfnu.edu.cn](mailto:jyd7785@qfnu.edu.cn) (Y. Jing).

In terms of WY evaluation, the existing studies mostly adopt two methods for quantitative evaluation: value-based and physical quantity evaluation (Ellison et al., 2012). The calculation method based on value is relatively subjective and fails to reflect the contribution of ecosystem service to the environment. The physical quantity evaluation method is to evaluate the services provided by the ecosystem as a whole from the perspective of physical quantity, independent of the impact of service pricing factors, and can objectively reflect the structure, function, and ecological process of the ecosystem (Zhang et al., 2018). With the development of 3S technology, model methods for physical quantity evaluation have become mature. Some multi-modal and integrated ecological hydro-logical models have been applied in ecosystem service evaluation, mainly including SWAT model (Aghsaei et al., 2020; Zhao et al., 2023); ARIES model (Capriolo et al., 2020); InVEST model (Bai et al., 2019), etc. The InVEST model has several advantages such as requiring fewer demand data, fast operation speed, and high accuracy (Shen et al., 2021; Xu et al., 2021), and can realize visual mapping of spatial distribution and dynamic changes in WY, indicating the influence of LULC change on WY (Chen et al., 2020; Sun et al., 2020). The InVEST model has been applied by more domestic and foreign scholars in regional WY evaluations.

Forecasting the possible implications of long-term LULC change on the WY of the ecosystem is crucial for formulating rational and timely ecological protection plans in advance. Cellular automata (CA)-Markov (Leta et al., 2021; Lu et al., 2019), CLUE-S (Gao et al., 2021; Islam et al., 2021), and FLUS (Zhang et al., 2020) are widely used in current LULC change prediction models. The above prediction models have focused on improving modeling techniques, regulations and accuracy of the models, but little research has been done to exploring of the potential driving forces that affect LULC change (Buhne et al., 2021). More importantly, it is difficult to identify the potential driving forces of LULC change and to capturing the evolution of multiple types of LULC patches in a dynamic way, especially natural land type patches. To address these issues, Liang Xun et al. (Liang et al., 2021) proposed the PLUS model. The PLUS model integrates a land expansion analysis strategy (LEAS) and a cellular automata model utilizing multiple types of randomly seeded patches (CARS) with strong data mining and patch-level dynamic simulation capabilities of LULC. In contrast to existing models, the PLUS model can dig better into the causal factors of each type of LULC change and more effectively simulates changes at the patch-level of multiple types of LULC. If LULC planning policies are involved in the simulation process and coupled with multi-objective optimization algorithms, the simulation results will be more similar to the real situation and have higher reference significance. Therefore, it has been applied in numerous areas such as optimal allocation of land resources and delimitation of urban expansion boundaries (Zhang et al., 2022).

Previous land prediction models utilized a bottom-up approach to assign each land type to an appropriate location but relied on their individual transformation principles and are devoid of optimized LULC structures. Fewer studies have been conducted on LULC optimization from the perspective of improving the comprehensive benefits of LULC. Few studies explored LULC optimization using multi-objective optimization scenario combination prediction models that analyze LULC quantity, spatial layout, and collaborative optimization of benefits (Li et al., 2021). While the InVEST and PLUS models have been coupled to predict future spatial-temporal distribution patterns of LULC, few studies have applied them to investigate the future trend of regional WY (Huang et al., 2019). To address the above shortcomings, we developed the GMOP-PLUS-InVEST (GPI) coupling model, which combines the strengths of the three models with respect to quantitative prediction and spatial structure (Du et al., 2022). Using the GPI coupling model, we realized the majorization of future LULC quantitative and spatial optimization for different scenarios, compensating for the inadequacy of the single aspect of quantitative or spatial optimization of LULC. Furthermore, it enhanced the reliability of future scenario setting, thereby improving the estimation precision of future LULC optimization and WY.

The Nansi Lake Basin (NLB) is situated in the Southern Shandong Economic Circle of China. In recent years, the economic level of the NLB has shown improvement, the industrialization and urbanization process has accelerated. However, due to the region's heavy responsibility of grain production, the contradiction between human and land has become increasingly prominent. To address this issue, the Department of Natural Resources of Shandong Province issued the "Special plan for ecological protection and restoration of the NLB (2021–2035)" in 2022. Hereinafter referred to as "Special plan (2021–2035)". This plan aims to build an ecological pattern of "one core, one screen, two belts, three zones, and multiple corridors" to achieve the development goal of creating an excellent ecological environment in the NLB characterized by "green mountains, clear water, lush forests, fertile fields, and beautiful lakes". In light of this, the objective of this study was to establish three scenarios: business as usual (BAU), economic development scenario (ED), and ecological conservation scenario (EC), using the GPI coupling model, anticipate the future distribution of LULC of the NLB, evaluate its WY, and analyze how the WY is spatially correlated. Specifically, the following objectives were addressed: (1) Identify the spatial-temporal changes in LULC of the NLB from 2000 to 2020. (2) Make quantitative predictions and spatial simulation of the LULC in the NLB under three scenarios (BAU, ED, EC) in 2035. (3) Evaluate the spatial-temporal changes and spatial correlation of WY of the NLB from 2000 to 2035. Overall, this study reveals the influence of LULC changes on WY, and provides a reliable scientific proof and reference for the rational development of land resources and restoration of ecological environment in the basin.

## 2. Study area and data sources

### 2.1. Study area

Nansi Lake, situated at the junction of Shandong and Jiangsu provinces, is composed of four interconnected lakes, namely Weishan Lake, Zhaoyang Lake, Dushan Lake, and Nanyang Lake. It is the largest freshwater lake in northern China (Fig. 1). The NLB is characterized by four distinct seasons and rain heat synchronization, with an average annual precipitation of 695.20 mm and an average annual temperature of 13.70 °C. The basin possesses about 7.07 billion m<sup>3</sup> of water resources, accounting for about 19.00% of the total water resources in Shandong province. Nansi Lake Nature Reserve was approved as a provincial nature reserve by Shandong Provincial Government in 2003. The waterway within the Nansi Lake and the Beijing-Hangzhou Grand Canal has played a significant role in promoting the economic development. The NLB is an important production base for grain, cotton, energy, and freshwater fishery in Shandong Province and even in China. The overall terrain of the basin slopes from west to east. The LULC structure is overwhelmingly dominated by farmland and construction land. Presently, the conflict between availability and demands of land resources in the NLB is increasingly acute. The total amount of forest and grass resources has decreased, the degradation and occupation of wetland resources are prominent, and the topography and landscape have severely degraded.

### 2.2. Data sources

Various data sources encompassed LULC, natural environment, socioeconomic, accessibility factors, etc. were used in this study. (Table 1). The LULC data (2000, 2010, 2020) were extracted from China's 30-meter annual land cover dynamic dataset spanning from 1990 to 2020 (<https://doi.org/10.5281/zenodo.5816591>). Through the utilization of ArcGIS software, LULC types had been reclassified into six categories: farmland, forestland, grassland, water area, construction land, and unused land.

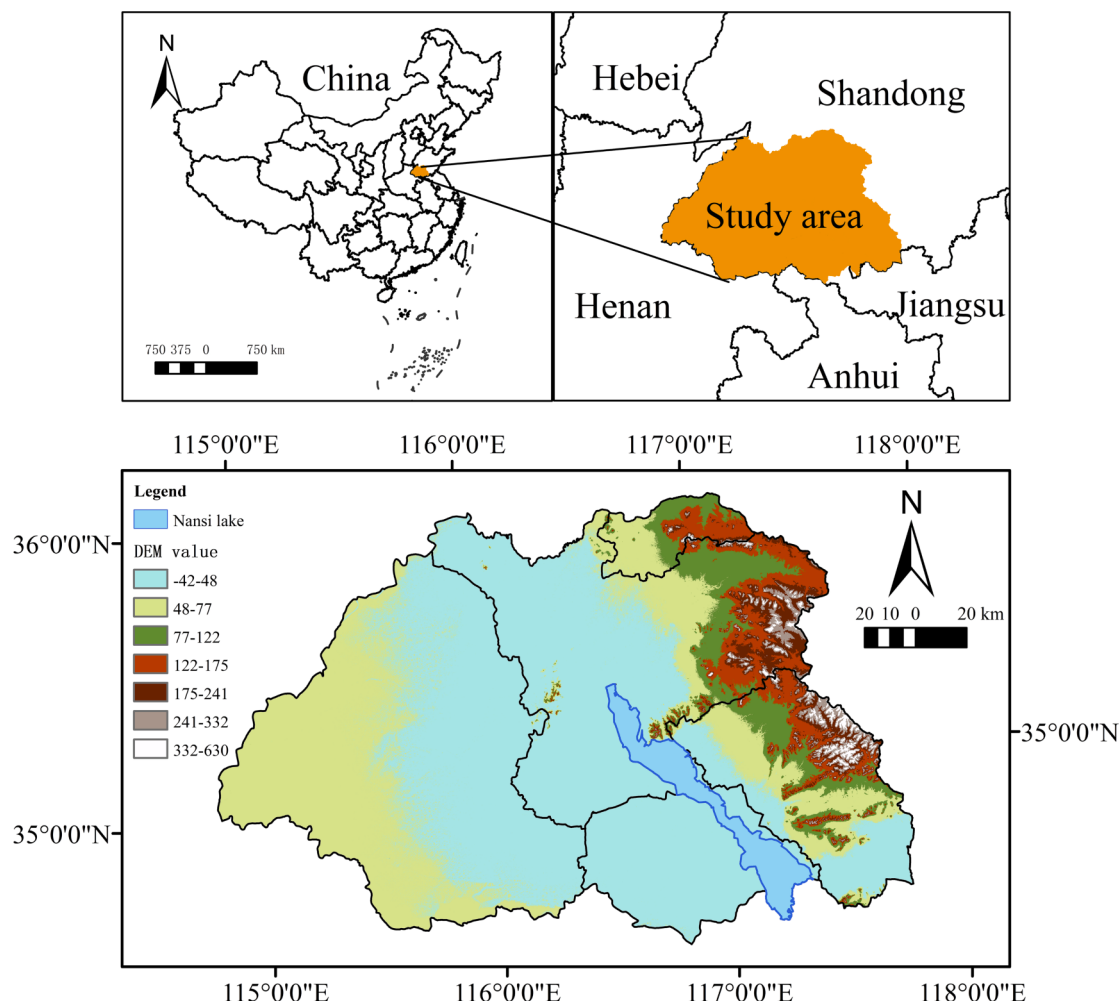


**Fig. 1.** Geographical location and elevation of the study area.

**Table 1**  
Main data sources in this study.

Data type	Data name	Data source
LULC data	LULC in 2000, 2010 and 2020	Dynamic data set of land cover in China for 30 years from 1990 to 2020 ( <a href="https://doi.org/10.5281/zenodo.5816591">https://doi.org/10.5281/zenodo.5816591</a> )
Natural environment	Elevation	Geospatial data cloud ( <a href="https://www.gscloud.cn">https://www.gscloud.cn</a> )
	Aspect	Elevation-based extraction
	Average temperature, average precipitation	Resource and Environmental Science Data Center of Chinese Academy of Sciences ( <a href="https://www.resdc.cn">https://www.resdc.cn</a> )
	Soil type	China Soil Data Set (1:1 million)
	Potential evapotranspiration	Global drought index and potential evapotranspiration database ( <a href="https://cgiarcsi.community">https://cgiarcsi.community</a> )
Accessibility factor	Distance from main river, distance from main railway	Resource and Environmental Science Data Center of Chinese Academy of Sciences ( <a href="https://www.resdc.cn">https://www.resdc.cn</a> )
Socioeconomic data	Population density, gross domestic product (GDP), grain output/price, etc	Statistical yearbook, statistical bulletin, national agricultural product cost-benefit data compilation (2020), etc
Policy constraints	Open water surface	Resource and Environmental Science Data Center of Chinese Academy of Sciences ( <a href="https://www.resdc.cn">https://www.resdc.cn</a> )

### 3. Methods

The research framework used in this study can be broken down into three main components (Fig. 2). Initially, simulation of quantitative LULC demand in 2035 under different scenarios was obtained utilizing the linear regression and the GMOP model. Subsequently, the amount of future LULC was allocated to a reasonable location according to spatial needs using the PLUS model. Lastly, the WY module of the InVEST model was deployed to assess the alterations in WY.

#### 3.1. Optimization of LULC structure based on GMOP

The GMOP model is an innovative approach that combines and advances the gray linear regression and multi-objective programming techniques. It not only accommodates the kinds of nondeterminacy in goal functions and restraint condition related to real-world LULC, but also addresses multi-objective issues during the optimization process of LULC structure (Du et al., 2022). The construction of this model involves four primary elements: selection of decision variables, establishment of objective functions, identification of gray constraints, and selection of solution methods.

##### 3.1.1. Decision variables

In this study, the setting of decision variables was selected in consideration of data availability and operability of the NLB. Six decision variables were selected, including farmland, forestland, grassland, water area construction land, and unused land.

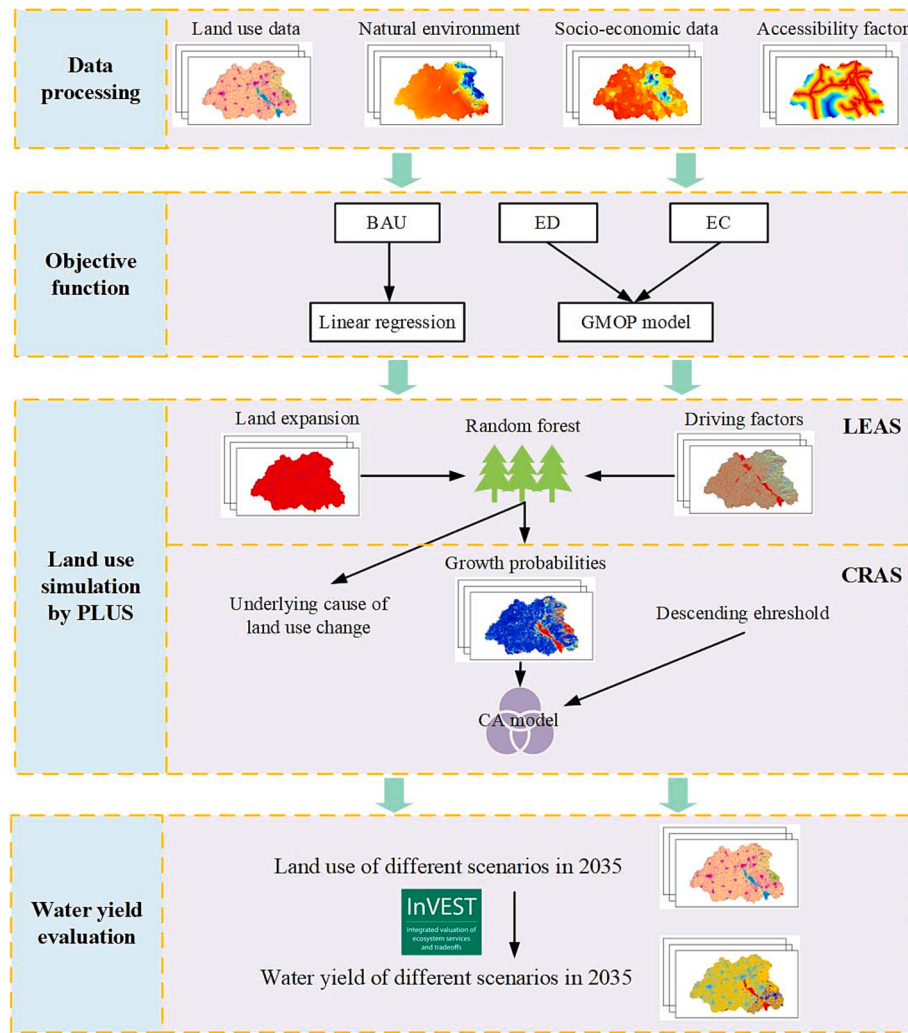


Fig. 2. Research framework of the study.

### 3.1.2. Scenario settings

BAU: Based on the probability matrix of land transfer from 2000 to 2020, the quantitative demand for various LULC types in 2035 was calculated using linear regression.

ED: The economic benefit objective function is:

$$F_1(x) = \max \sum_{j=1}^n c_j x_j \quad (1)$$

where  $F_1(x)$  is the economic benefit;  $c_j$  is the economic benefit per unit area of each decision variable, and  $x_j$  is the decision variable.

Using GM (1,1) model, it was predicted that the economic benefits per unit area of farmland, forestland, grassland, water area, and construction land in the target year are  $5.95/\text{hm}^2$ ,  $5.74/\text{hm}^2$ ,  $41.9/\text{hm}^2$ ,  $6.61/\text{hm}^2$ , and  $150.16/\text{hm}^2$ , respectively. Because the economic benefits of unused land were not obvious, the economic benefits of unused land were set at  $0.01/\text{hm}^2$ . Finally, the economic benefit objective function coefficient of the NLB was obtained (unit:  $10,000 \text{ yuan}/\text{hm}^2$ ):

$$\text{Max } (x) = 5.95x_1 + 5.74x_2 + 41.90x_3 + 6.61x_4 + 150.16x_5 + 0.01x_6$$

EC: Set target functions to maximize the total ecosystem service value (ESV) supplied by all LULC types. The ecological benefit objective function is:

$$F_2(x) = \max \sum_{j=1}^n d_j x_j \quad (2)$$

where  $F_2(x)$  is ESV;  $X_j$  is the decision variable of j LULC type ( $x_{1-6}$  represents farmland, forestland, grassland, water area, construction land, and unused land, respectively);  $D_j$  represents the ESV per unit area.

This study used ESV to characterize ecological benefits. To reduce errors, based on the “Unit Area ESV Equivalency Table” (Xie et al., 2015), the ESV coefficients for various categories had been revised with combination the results of previous studies of the NLB (Wang et al., 2022a). Construction land was not considered. According to the unit area grain economic output value predicted by GM (1,1) model in the target year, the ESV coefficient table per unit area of the NLB was calculated (Table 2). The ecological benefit objective function of each decision variable in the NLB was (unit:  $10,000 \text{ yuan}/\text{hm}^2$ ):

$$\text{Max } (x) = 0.84 x_1 + 4.10x_2 + 2.52 x_3 + 26.20 x_4 + 0 x_5 + 5.42x_6$$

### 3.1.3. Constraint setting

(1) Total land

$$x_1 + x_2 + x_3 + x_4 + x_5 + x_6 = 3171788.64 \quad (3)$$

(2) Population

The population of the construction land should be controlled within the target predicted population range of the study area:

$$m \times x_5 \leq P \quad (4)$$

where  $m$  is the average population density of the construction land, and  $P$  is the total population.

**Table 2**

ESV coefficients of LULC categories in the NLB.

LULC type	Farmland	Forestland	Grassland	Water area	Construction land	Unused land
ESV coefficient	0.84	4.10	2.52	26.20	0	5.42

The gray GM (1,1) model was used to forecast the average population density and total population of construction land in 2035, determining  $m = 13.58$ ,  $P = 1012234$ .

### (3) Farmland

According to the requirements of “grain for green” and “returning farmland to grassland” in the “Special plan (2021–2035)”, while strictly observing the arable land minimum, the area of basic farmland in various regions was protected to guarantee the growth of the agricultural economy. The farmland area should be smaller than the status quo and larger than the arable land minimum:

$$1823040.00 \leq x_1 \leq 2308737.33 \quad (5)$$

### (4) Forestland

According to the requirements of “grain for green” in the “Special plan (2021–2035)”, the proportion of forests should be increased. To ensure ecological construction and increase forest coverage, the area of forestland of the NLB in 2035 should not be smaller than the current situation:

$$38376.09 \leq x_2 \quad (6)$$

### (5) Grassland

From 2000 to 2020, the total grassland area decreased year by year and was mainly converted into farmland. According to the requirements of “returning farmland to grassland” in the “Special plan (2021–2035)”, the percentage of grassland needs to be improved. In conjunction with the economic development requirements of the NLB, the grassland area should be maintained below the grassland area in 2000:

$$20081.07 \leq x_3 \leq 43611.03 \quad (7)$$

### (6) Water area

From 2000 to 2020, the water area of Nansi Lake changed significantly. To coordinate the balanced development of economy and ecology, the peak value of water area for nearly 20 years was set as the lower limit, and the valley value was set as the upper limit:

$$108713.52 \leq x_4 \leq 125032.95 \quad (8)$$

### (7) Construction land

In the light of the “Special plan (2021–2035)”, taking urbanization process and economic development requirements into account, the construction land area of the NLB in 2035 should be at least larger than the current situation:

$$695793.15 \leq x_5 \quad (9)$$

### (8) Model self-constraint

$$x_i \geq 0, i = 1, 2, 3 \dots 6 \quad (10)$$

#### 3.1.4. Solution

Solve the functions of the above constraints using Lingo 18 software and ultimately obtain the land demand quantity for the multi-objective optimization scenarios in 2035.

#### 3.2. Optimization of spatial LULC structure based on PLUS

CA model exhibits inadequacies in both conversion rule mining strategies and simulation strategies for landscape dynamic change. Therefore, this study utilized the PLUS model which encompasses both LEAS and CARS to simulate future LULC changes. LEAS provides the ability to dissect the dynamics of LULC change over a certain period of time with enhanced explanatory power, whereas CARS blends a random

seed generation mechanism with a threshold reduction mechanism to automatically generate spatial-temporally dynamic simulated patches within the restraints of probability of occurrence.

#### 3.2.1. Model input

To estimate the appropriate probability of different LULC types, this study utilized LULC data from two phases to obtain LULC extension map. In accordance with the natural environment, socioeconomic development of the research area, previous studies (Ding et al., 2022), and data availability, a total of 9 driving factors of LULC change were selected (Fig. 3), including 5 natural factors (elevation, aspect, annual average temperature, annual average precipitation, and soil type), 2 socioeconomic factors (GDP and population density), and 2 accessibility factors (distance from railways and rivers). Neighborhood factors reflect the interactions between distinct LULC types and within different LULC units in the vicinity. The parameter values for neighborhood factors in this paper were determined reference to the historical characteristics of LULC change in the NLB (Jing et al., 2021): farmland (0.4), forestland (0.7), grassland (0.6), water area (0.8), construction land (0.9), and unused land (0.3).

#### 3.2.2. Accuracy verification

By utilizing LULC data and driving factor data in 2010 and 2020, this study adopted the PLUS model to make simulations of LULC landscape pattern of the NLB in 2020. Through a comparison between the actual and simulated results, it was found that the overall accuracy reached 0.92, with a Kappa coefficient of 0.81. These results demonstrate that the PLUS model exhibited excellent simulation accuracy for the research area and is highly reliable and applicable. Based on this, the study anticipated and analyzed LULC under diverse scenarios in 2035 via the LULC data for 2020.

#### 3.3. Evaluation of WY changes

To assess the WY of the NLB, we employed the WY module of the InVEST model in this study. The Budyko water heat coupling equilibrium hypothesis and annual average precipitation data were utilized to determine the annual WY Y of each grid unit  $x$  in the NLB (Wang et al., 2022c) using the following formula:

$$Y(x) = \left\{ 1 - \frac{AET(x)}{P(x)} \right\} \times P(x) \quad (11)$$

where  $AET(x)$  represents the actual annual evapotranspiration of grid unit  $x$ , and  $P$  represents the annual precipitation of grid unit  $x$ .

In the water balance formula, the vegetation evapotranspiration for LULC types was calculated using the formula:

$$\frac{AET(x)}{P(x)} = 1 + \frac{PET(x)}{P(x)} - \left[ 1 + \left\{ \frac{PET(x)^{\omega}}{P(x)} \right\} \right]^{1/\omega} \quad (12)$$

where  $PET(x)$  represents the potential evapotranspiration,  $\omega$  non-physical parameters that represent the natural climate-soil properties.

#### 3.4. Spatial relevance evaluation based on grid

To generate a grid of 3 km × 3 km consistent with the study area, we employed ArcGIS software. Subsequently, we linked the WY data to the grid to obtain the WY value for each unit area. Utilizing GeoDa software, the global auto-correlation results were obtained by first calculating

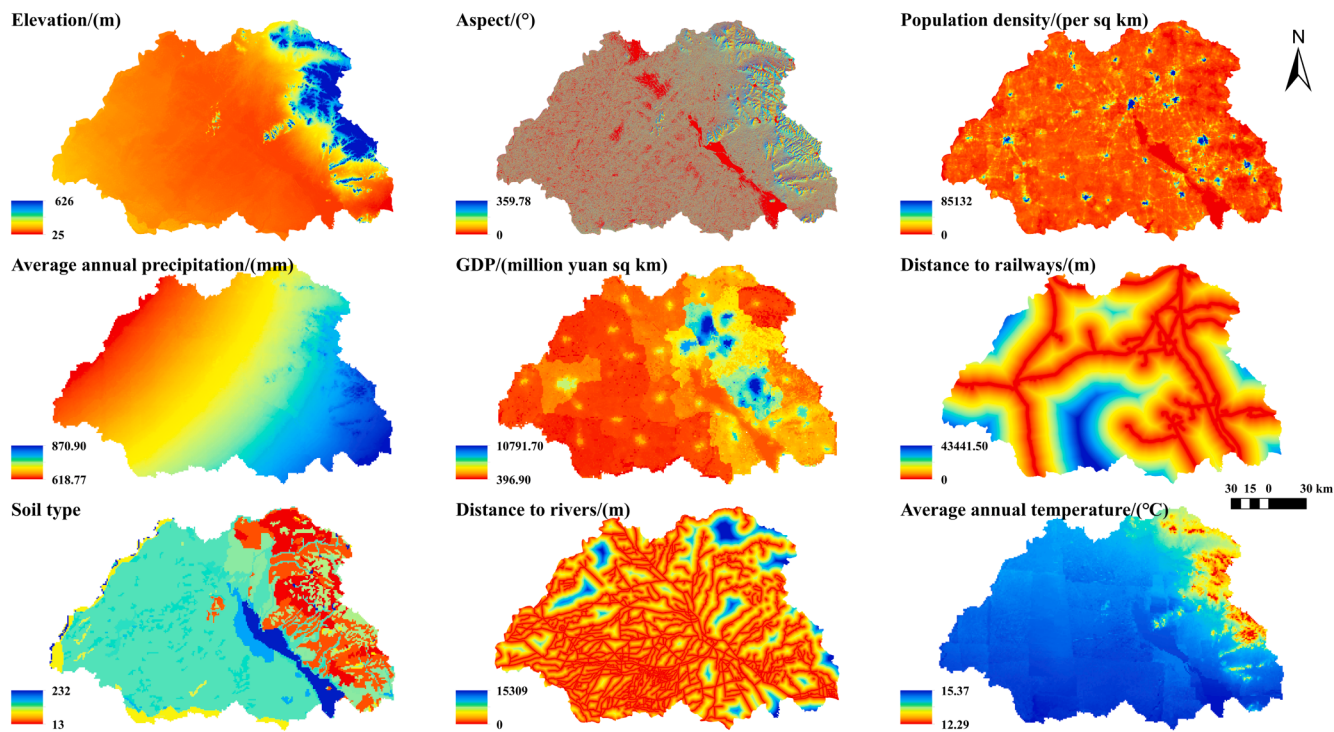


**Fig. 3.** Driving factors affecting LULC in the study area.

Moran's I value at the grid scale. The distribution of WY hot spots in the NLB was analyzed using Getis Ord Gi\*. Finally, local auto-correlation results and LISA aggregation graphs were obtained by utilizing Anselin Local Moran's I.

#### 4. Results

##### 4.1. Spatial-temporal changes in LULC in NLB

According to the findings presented in Table 3, farmland was the dominant LULC type in the NLB from 2000 to 2020, followed closely by construction land, while the rest of the LULC types together account for less than one-fifth. From the perspective of changing trends in LULC types (Fig. 4), it was observed that farmland and grassland exhibited a continuous and significant decline over the past two decades, with grassland experiencing a particularly pronounced reduction. Specifically, the grassland change rates were 22.40% and 40.65% in 2000–2010 and 2010–2020, respectively, resulting in a sharp decrease in area from 436.11 km<sup>2</sup> in 2000 to 200.81 km<sup>2</sup> in 2020. In contrast, there was an upward trend in construction land and forestland, with forestland experiencing a notable increase from 2010 to 2020, reaching 34.73%. Although there was a significant expansion of water area in the NLB, the proportion of unused land was minuscule and will not be discussed in this analysis.

According to Fig. 5, the spatial layout of LULC in the NLB had changed significantly from 2000 to 2020. Farmland was widely distributed, primarily concentrated in the western plain region west of

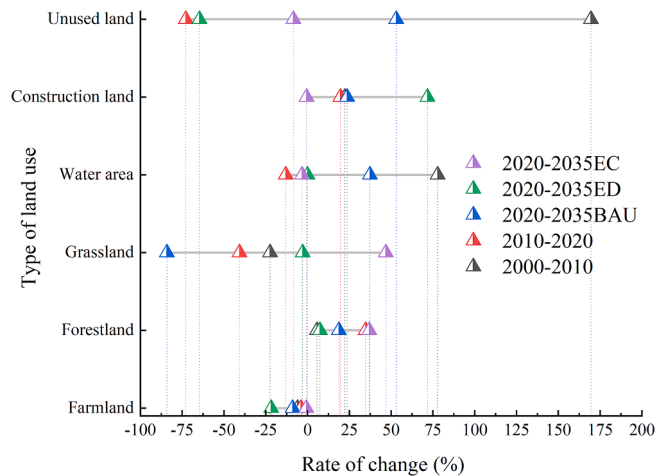


**Fig. 4.** Changes in LULC types in the study area from 2000 to 2035. 2020-EC represents the changes in the EC scenario from 2020 to 2035, and the rest are the same.

Nansi Lake. Except for sporadic distribution in the middle and south parts of the NLB, forestland and grassland were concentrated in the eastern part of the hilly mountainous area with high altitude in the eastern part of the NLB. In response to the rapid economic development

**Table 3**

Areas of LULC types in the study area from 2000 to 2020 and predictions for 2035 under different scenarios (km<sup>2</sup>).

Year	Farmland	Forestland	Grassland	Water area	Construction land	Unused land
2000	25557.09	269.52	436.11	702.91	4751.04	1.19
2010	24029.23	284.83	338.38	1250.32	5811.93	3.22
2020	23087.37	383.76	200.81	1087.13	6957.93	0.87
2035BAU	21033.76	455.80	31.82	1493.01	8606.50	1.33
2035ED	18067.59	412.17	194.92	1090.91	11951.97	0.30
2035EC	22924.56	525.57	294.91	1051.93	6919.08	0.80

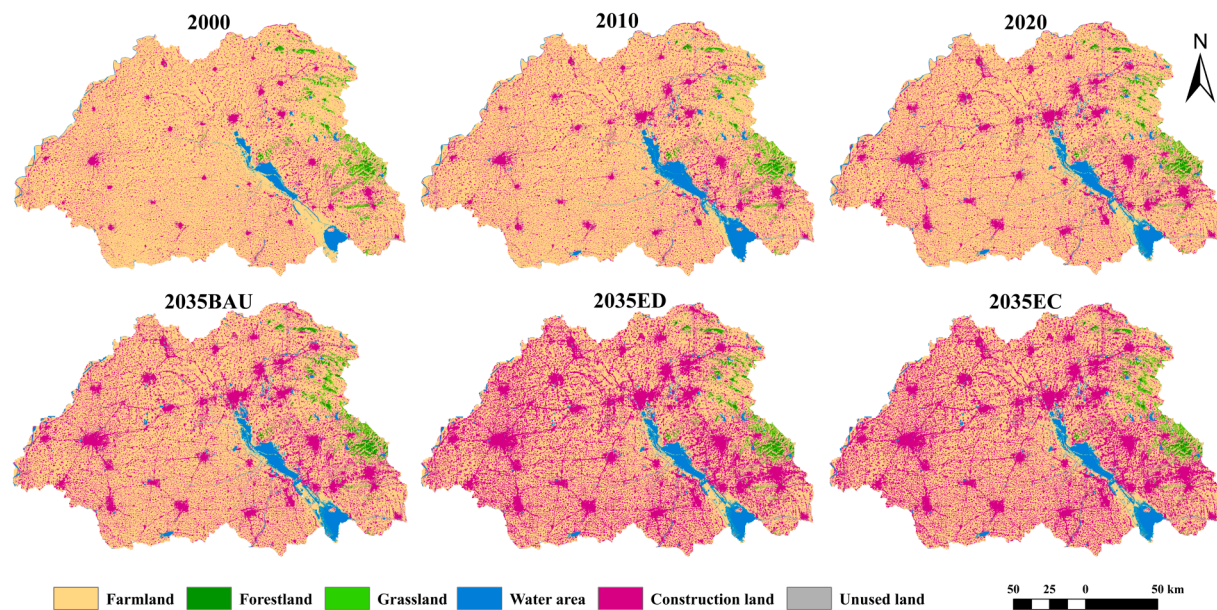


Fig. 5. Spatial distribution characteristics of LULC in the study area.

of the NLB, construction land expanded in all directions, encroaching on surrounding farmland and grassland. Of note, the most significant changes occurred in the middle areas of Jining City, Heze City Mudan District, and Zaozhuang City. Overall, the 20-year period witnessed complex transfers between all LULC types in the NLB, with the most prominent changes observed in farmland and construction land. These alterations arose largely from the rapid pace of urbanization and the implementation of policies such as “two refunds and three repayments” (returning farmland and ponds, repaying forests, wetlands, and lakes) and residential renovation programs aimed at ensuring the total amount of farmland.

#### 4.2. Multi-scenario simulation based on PLUS

According to Table 3, in the NLB, the structural proportion order of LULC types remained unchanged under three different scenarios in 2035. Farmland and construction land continued to dominate, followed by water area, forestland, grassland, and unused land. Rely on perspective of changing trends in LULC types (Fig. 4), under the BAU, the trend of farmland and construction land as the dominant LULC types in 2020–2035 was consistent with 2000–2020. Farmland continued to decline, while construction land continued to rise, with a more substantial and stable change compared to farmland. Forestland and grassland also exhibited trends similar to those observed over the past 20 years. Grassland continued to decline in both area and rate of decrease, while the increase in forestland slightly decreased. Under the ED, LULC types with the highest number of transfers continued to be farmland and construction land. Compared to the BAU, the percentage of decrease in farmland increased from 8.84% to 21.74%, and the change in construction land was more significant, with a sharp increase from approximately 20.00% to 71.77%. Meanwhile, compared to the year 2020, the water area and grassland under the ED exhibited almost no change, and the percentage of increase in forestland decreased from 34.73% to 7.40% between 2010 and 2020. Under the EC, forestland and grassland experienced substantial increases, reaching 36.95% and 46.86%, respectively, compared to the year 2020. Other land types, including farmland and construction land, exhibited minimal changes, with no continuation of trends observed over the past 20 years.

#### 4.3. Contribution rate of driving factors for LULC expansion

The LEAS and CARS are the central components of the PLUS model. The LEAS uses a built-in random forest regression training process to provide directly quantitative information on how the various drivers affect the extent of the contribution of each LULC type to the expansion. This information helps us understand the potential causes of LULC change. Fig. 6 shows that elevation is the most significant driving factor contributing to LULC change in the NLB. It ranks first among all driving factors for the expansion of farmland, forestland, grassland, and unused land. For water areas and construction land, elevation ranks second and third, respectively. In particular, elevation has the highest contribution rate of 0.2993 for grassland expansion, which is much higher than other driving factors. The annual average precipitation ranks second with only a contribution rate of 0.1292. For forest expansion, natural factors play a dominant role, with the top three contributing factors being elevation, aspect, and annual average temperature.

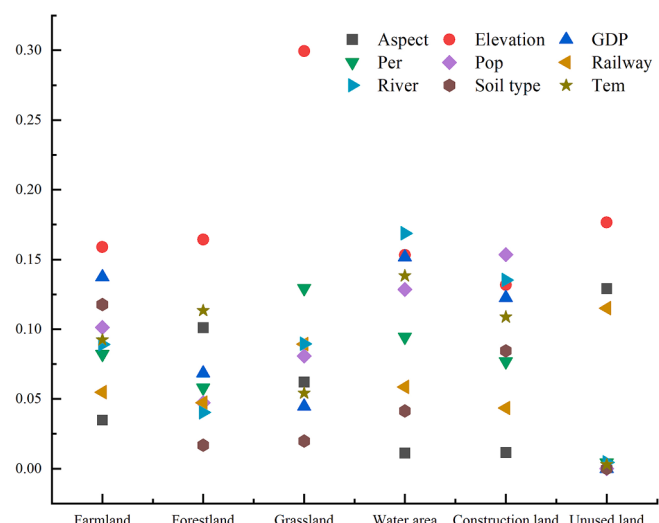


Fig. 6. Driver contribution rate in the study area. Abbreviation: Per: annual average precipitation; Pop: population density; Railway: distance to the railway; River: distance to the river; Tem: annual average temperature.

#### 4.4. Evaluation of WY change based on InVEST

The InVEST model was utilized to assess the changes in WY in the NLB by inputting the LULC simulation results in 2000, 2010, 2020, and different scenarios in 2035 (Fig. 7). The study found that WY was mainly affected by LULC types, with construction land exhibiting high values and water area having low values. In terms of spatial distribution, extreme high values were observed in the southeast corner of the NLB. Based on zoning statistics by ArcGIS 10.8, a comprehensive assessment of WY was conducted for each county in the NLB (Fig. 8). However, the central district of Jining City and the Nansi Lake had relatively single LULC types – mainly consisting of construction land or water area – which resulted to their WY always showcasing extreme high or low values. Thus, these values were not taken into account during the analysis. During the period between 2000 and 2020, the NLB witnessed a continuous increase in WY. At the beginning of 2000, the WY of each county was relatively low, with the exception of the central district of Zaozhuang City, which exhibited a distribution pattern of high-south and low-north. By 2010, except for Ningyang County and Dongming County, all the “north low” counties had transformed into “south high” counties, and the WY of Pei County, Tengzhou City, Xuecheng District, and Zaozhuang City had entered a higher level than before. Compared to 2010, the WY in all counties and districts in 2020 had increased, except for the central district of Zaozhuang City, which remained unchanged. In 2035, the WY in the NLB had increased compared to 2020, with ED > EC > BAU. The overall distribution pattern displayed that the south was significantly higher than the north and the east was significantly higher than the west. High values were concentrated in Tengzhou City, Xuecheng District, Yicheng District, and Zaozhuang City, which are located towards the east of Nansi Lake. The increase in WY is attributed to the anticipated expansion of construction land, regardless of the scenario. The distribution pattern of WY is primarily influenced by precipitation, which remains relatively stable across the NLB. Precipitation levels are highest in the southeast and lowest in the northwest, consistent with observed patterns of WT.

#### 4.5. Spatial correlation of WY in NLB

From a spatial correlation perspective, the Moran's I value of WY in the NLB from 2000 to 2020 and under different scenarios in 2035 were all greater than 0, with values of 0.395, 0.500, 0.496, 0.593, 0.617, and

0.612 respectively. This result indicates that the territorial distribution of WY in the NLB exhibited certain clustering phenomena. Through Getis-Ord Gi\* analysis, significant clustering regions can be identified. These are locations where high or low value elements cluster spatially, with cold and hot spots representing low and high values respectively. The Getis-Ord Gi\* analysis (Fig. 9) indicated that there were no significant changes in the region of cold and hot spots in WY in the last two decades. The hot spots were mainly located in urban areas with predominantly construction land, with Mudan District, Jining City Central District, Zaozhuang City Central District, Xuecheng District, and Pei County being more prominent, while the cold spots were clustered in the Nansi Lake. In 2035, the distribution of cold and hot spots for WY under different scenarios still exhibited characteristics similar as from 2000 to 2020. However, hot spots increased significantly and were interconnected in Tengzhou City, Xuecheng District, and Zaozhuang City, which are located west of Nansi Lake. Cold spots aggregated in the eastern hilly area of the NLB. At the same time, the LISA cluster diagram (Fig. 10) revealed that the distribution of high-high concentration areas of WY was highly consistent with that of hot spots, and the counties and districts around the Nansi Lake were more prominent. A high-high concentration area refers to an area with high value both in itself and its surroundings, while a low-low concentration areas is the opposite. The low-low concentration areas of WY were concentrated in the Nansi Lake and the eastern hilly area and banded distribution near the northwest border of the basin. From 2000 to 2020, the LISA cluster diagram of water yield in the NLB exhibited limited and irregular changes, with various transitions occurring. Significant increases occurred in the transition from insignificant areas to other situations under different scenarios in 2035, resulting in a more pronounced agglomeration phenomenon characterized by an increase and merging of high-high concentration areas and low-low concentration areas in the eastern part of the NLB. It is worth noting that Dongming County transformed from a low-low concentration area in 2000–2020 to an insignificant area in 2035.

## 5. Discussion

The results of the study showed that LULC transfers were occurring all the time in the NLB from 2000 to 2020, with farmland and construction land being the most significant (Wang et al., 2022a). Under the BAU, if no intervention were made, the expansion of construction land

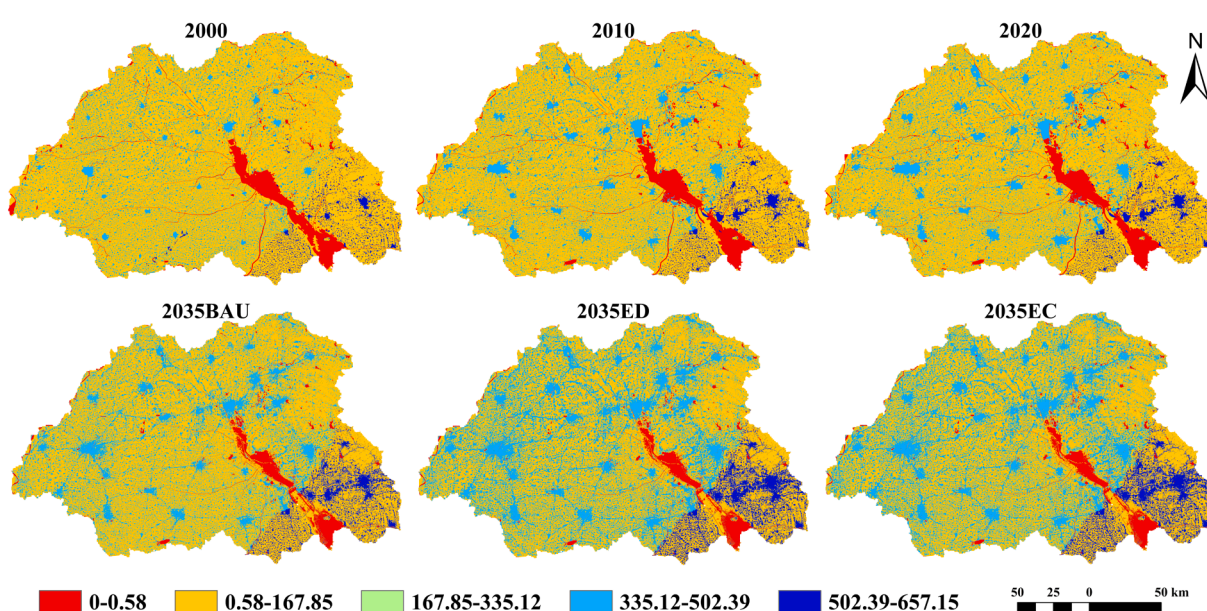


Fig. 7. WY in the study area from 2000 to 2035.

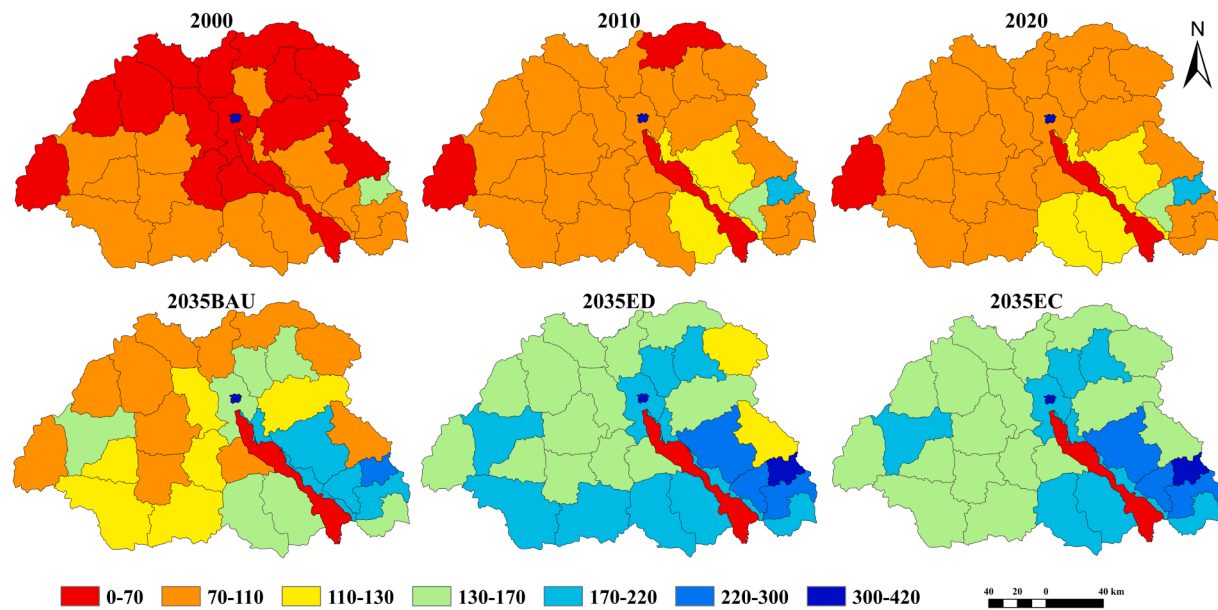


Fig. 8. WY of every district in the study area from 2000 to 2035.

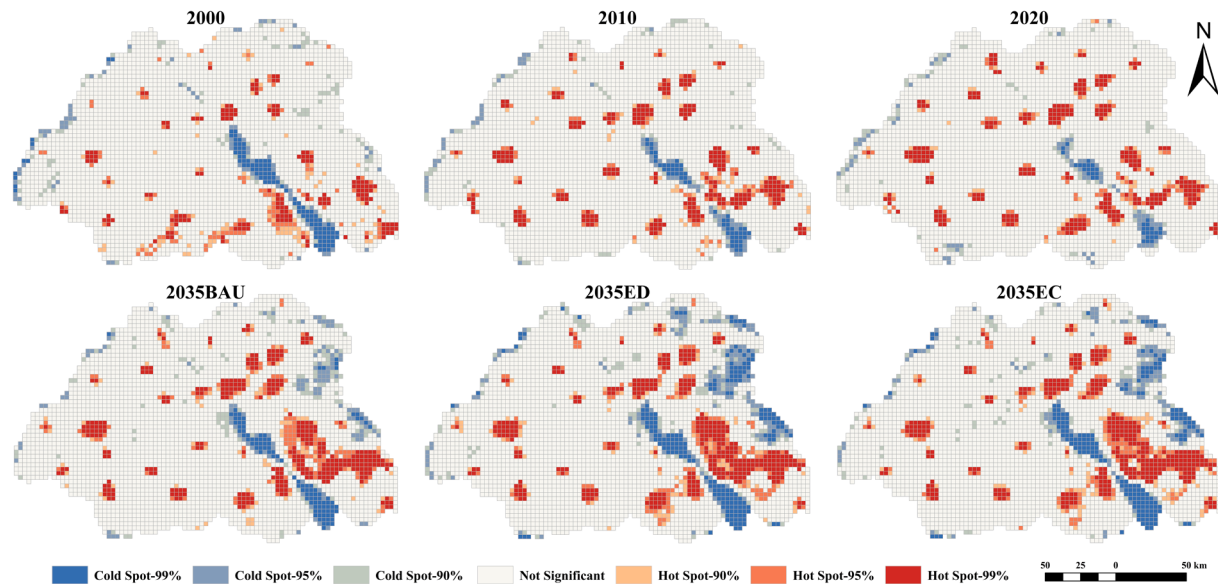


Fig. 9. Distribution of WY hot spots map in the study area from 2000 to 2035.

encroaching on farmland, especially in mountainous and urban areas, would continue to be the main feature of future LULC changes. However, policies, regulations, and other factors play a crucial role in shaping LULC change, which directly affects the future development of LULC. By inputting the development goals and requirements of the “Special plan (2021–2035)” into the GMOP model as constraints, and constructing the ED and EC, the research found that different policy orientations and development goals had significant impacts on the trends of LULC change. Specifically, the results of the LULC simulation in 2035 revealed that grassland and construction land responded more significantly to these policy changes (Fig. 4).

Based on the results of LULC simulation in the NLB in 2035, evaluation results of the InVEST model revealed that a significant increase in WY under three different scenarios, with the highest WY observed under the ED and the lowest under the BAU (Fu et al., 2018). These results indicate that LULC change has a significant effect on WY. Using the GPI coupling model to optimize the LULC structure can help reconcile the

conflict between land resource utilization and socioeconomic development in the basin. Construction land has a significant contribution to WY in the NLB, and this impact showed a positive correlation. Previous studies (Guo et al., 2016) have also shown that construction land has a promoting effect on WY. This may be due to the fact that the underlying surface of most construction land is impermeable, which impedes infiltration and increases surface runoff. Consequently, construction land has a high capacity of WY, indicating that the WY of construction land is significantly higher than that of other LULC types (Fig. 6). Comparing the annual average precipitation (Fig. 3) and WY (Fig. 6) in the NLB, it was found that the WY of construction properties was high in the southeast part of the basin and low in the northwest region. This distribution pattern was highly consistent with that of the annual average precipitation. This suggests that precipitation is the primary source of water for runoff formation and is the basic condition that determines the WY (Li et al., 2021).

Policies and regulations in different periods have a direct impact on

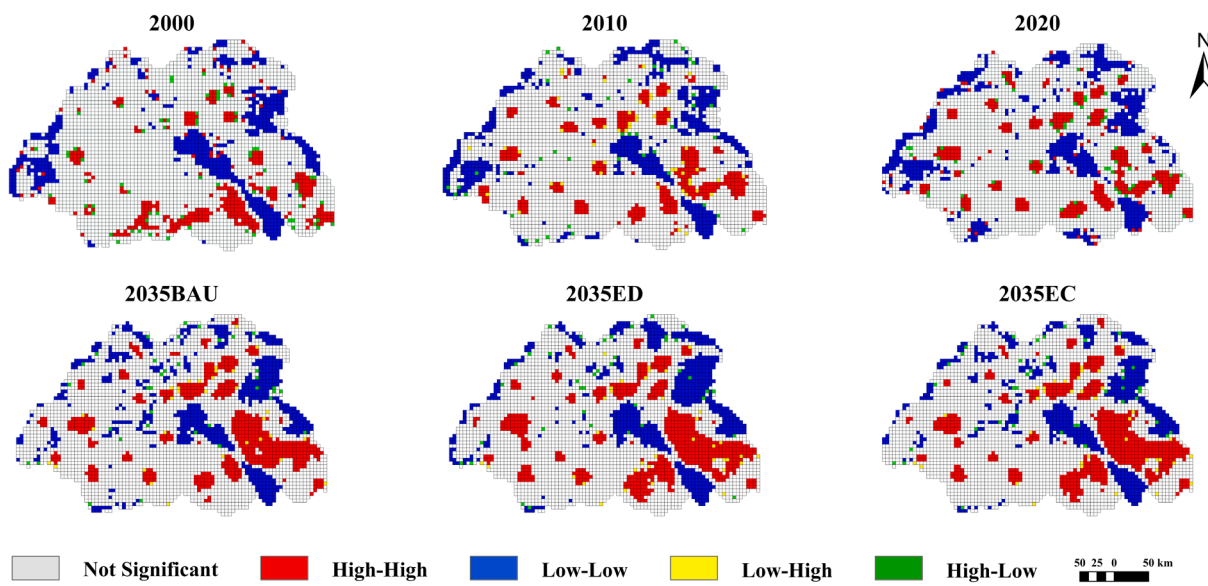


**Fig. 10.** Distribution of WY LISA cluster in the study area from 2000 to 2035.

the direction of LULC, but most previous studies did not conduct a detailed analysis of policy scenarios when establishing simulation models (Reheman et al., 2023). In this study, we used linear regression to construct the BAU and inputted the development goals and requirements of the “Special plan (2021–2035)” into the GMOP model as constraints to build the ED and EC. These scenarios fully consider the multiple goals of economic, social, and ecological benefits, which are required for new urbanization, ecological civilization, and rural revitalization. Compared to existing LULC change simulation models, the PLUS model allows spatial-temporal modeling of different LULC patches in a dynamic way and can obtain LULC change patterns within specific time intervals, improving the accuracy of simulation results (Li et al., 2022). The InVEST model is already relatively mature and has strong applicability in China. It can evaluate and analyze various spatial-temporal indicators and detect dynamic distribution changes (Wang et al., 2023). The GPI model built in this study takes full advantage of the strengths of each individual model in quantitative prediction and spatial allocation.

This study provides a valuable case study for future LULC simulation and WY evaluation of the NLB, which is essential for subsequent evaluation and quantification and offers new perspectives for decision-makers. However, there are still some limitations to this study. Firstly, besides the BAU, only the ED and EC were considered, and they may not fully represent all practical situations. Further scenarios should be developed, considering different policy orientations and development goals. Secondly, the selection of drivers was not comprehensive enough, which may have limited our ability to better explore the underlying causes of LULC type expansion. Therefore, future studies should expand the range of driving factors to achieve higher scientific and accuracy of simulation. Lastly, although the GM (1,1) model used to forecast population and other data has proven to be highly accurate, there is still considerable uncertainty in the prediction results. We need to continue refining models and improving data quality to reduce these uncertainties.

## 6. Conclusion

In this study, we used the GPI coupling model to optimize the LULC layout in the NLB under different scenarios and to investigate its impact on WY. Our simulation results demonstrated that compared to the BAU and ED, the EC showed a decrease in construction land expansion rate while ensuring basic farmland, alleviating the conflict between

construction land and farmland, and increasing the proportion of ecological land, which is more aligned with the goals of the “Special plan (2021–2035)”. Our assessment of the spatial-temporal pattern of WY in the NLB helped to understand the consequences of LULC change on WY. By examining changes in WY, we can comprehend the comprehensive impact and relative importance of LULC change on it, helping to address LULC planning issues and provide ideas for LULC decision-making. Since entering the 21st century, construction land encroaching on farmland has been the main trend of LULC change in the NLB and has resulted in the most significant land conflict issue in the region. Balancing urban expansion while ensuring the minimum amount of arable land to guarantee food security is the primary challenge facing the basin presently. From the perspective of ecosystem service changes, reasonable LULC planning can have a positive impact on WY to some extent. Effective management practices can further help managers formulate more comprehensive spatial planning, thereby ensuring that the efficiency of land resource use in the NLB is improved and the ecological environment is restored. Although this study has certain limitations, the results are practical and policy-relevant and can provide a reference for LULC change and ecosystem service function planning in the NLB and other similar regions.

## Funding

This work was funded with support from the Humanities and Social Science General Project of the Ministry of Education, China [grant number 15YJAZH027].

## Declaration of Competing Interest

The authors declare that they have no known competing financial interests or personal relationships that could have appeared to influence the work reported in this paper.

## Data availability

Data will be made available on request.

## References

- Aghsaei, H., Dinan, N.M., Moridi, A., Asadolahi, Z., Delavar, M., Fohrer, N., Wagner, P. D., 2020. Effects of dynamic land use/land cover change on water resources and

- sediment yield in the Anzali wetland catchment, Gilan, Iran. *Sci. Total Environ.* 712, 11. <https://doi.org/10.1016/j.scitotenv.2019.136449>.
- Bai, Y., Ochuodho, T.O., Yang, J., 2019. Impact of land use and climate change on water-related ecosystem services in Kentucky, USA. *Ecol. Ind.* 102, 51–64. <https://doi.org/10.1016/j.ecolind.2019.01.079>.
- Balist, J., Malekmohammadi, B., Jafari, H.R., Nohegar, A., Geneletti, D., 2022. Detecting land use and climate impacts on water yield ecosystem service in arid and semi-arid areas. A study in Sirvan River Basin-Iran. *Appl. Water Sci.* 12 (1), 14. <https://doi.org/10.1007/s13201-021-01545-8>.
- Benra, F., De Frutos, A., Gaglio, M., Alvarez-Garretón, C., Felipe-Lucía, M., Bonn, A., 2021. Mapping water ecosystem services: Evaluating InVEST model predictions in data scarce regions. *Environ. Model. Softw.* 138, 15. <https://doi.org/10.1016/j.envsoft.2021.104982>.
- Buhne, H.S.T., Tobias, J.A., Durant, S.M., Pettorelli, N., 2021. Improving predictions of climate change-land use change interactions. *Trends Ecol. Evol.* 36 (1), 29–38. <https://doi.org/10.1016/j.tree.2020.08.019>.
- Caprioli, A., Boschetto, R.G., Mascolo, R.A., Balbi, S., Villa, F., 2020. Biophysical and economic assessment of four ecosystem services for natural capital accounting in Italy. *Ecosyst. Serv.* 46, 14. <https://doi.org/10.1016/j.ecoser.2020.101207>.
- Chen, X.C., Li, F., Li, X.Q., Hu, Y.H., Hu, P.P., 2020. Evaluating and mapping water supply and demand for sustainable urban ecosystem management in Shenzhen, China. *J. Clean. Prod.* 251, 11. <https://doi.org/10.1016/j.jclepro.2019.119754>.
- Ding, Y., Wang, L.Z., Gui, F., Zhao, S., Zhu, W.Y., 2022. ecosystem carbon storage in Hangzhou Bay area based on InVEST and PLUS Models. *Environ. Sci.* <https://doi.org/10.19674/j.cnki.issn1000-6923>.
- Du, Y., Li, X., He, X., Li, X., Yang, G., Li, D., Xu, W., Qiao, X., Li, C., Sui, L., 2022. Multi-scenario simulation and trade-off analysis of ecological service value in the Manas River Basin Based on Land Use Optimization in China. *Int. J. Environ. Res. Public Health* 19 (10), 6216.
- Ellison, D., Futter, M.N., Bishop, K., 2012. On the forest cover-water yield debate: from demand- to supply-side thinking. *Glob. Chang. Biol.* 18 (3), 806–820. <https://doi.org/10.1111/j.1365-2486.2011.02589.x>.
- Fu, Q., Hou, Y., Wang, B., Bi, X., Li, B., Zhang, X.S., 2018. Scenario analysis of ecosystem service changes and interactions in a mountain-oasis-desert system: a case study in Altay Prefecture, China. *Sci. Rep.* 8, 13. <https://doi.org/10.1038/s41598-018-31043-y>.
- Gao, Y., Wang, J.M., Zhang, M., Li, S.J., 2021. Measurement and prediction of land use conflict in an opencast mining area. *Resour. Policy* 71, 11. <https://doi.org/10.1016/j.resourpol.2021.101999>.
- Guo, H.W., Sun, X.Y., Lian, L.S., Zhang, D.Z., Xu, Y., 2016. Response of water yield function of ecosystem to land use change in Nansi Lake Basin based on CLUE-S model and InVEST model. *J. Appl. Ecol.* 27 (9), 2899–2906. <https://doi.org/10.13287/j.1001-9332.201609.039>.
- Huang, L., Liao, F.H., Lohse, K.A., Larson, D.M., Fragkias, M., Lybecker, D.L., Baxter, C.V., 2019. Land conservation can mitigate freshwater ecosystem services degradation due to climate change in a semiarid catchment: The case of the Portneuf River catchment, Idaho, USA. *Sci. Total Environ.* 651, 1796–1809. <https://doi.org/10.1016/j.scitotenv.2018.09.260>.
- Islam, S., Li, Y.C., Ma, M.G., Chen, A.X., Ge, Z.X., 2021. Simulation and prediction of the spatial dynamics of land use changes modelling through CLUE-S in the Southeastern Region of Bangladesh. *J. Indian Soc. Remote Sens.* 49 (11), 2755–2777. <https://doi.org/10.1007/s12524-021-01402-w>.
- Jing, Y.D., Chang, Y.Q., Cheng, X.Y., Wang, D., 2021. Land-use changes and ecosystem services under different scenarios in Nansi Lake Basin, China. *Environ. Monitor. Assess.* 193 (1), 14. <https://doi.org/10.1007/s10661-020-08797-y>.
- Leta, M.K., Demissie, T.A., Traenckner, J., 2021. Modeling and prediction of land use land cover change dynamics based on land change modeler (LCM) in Nashe Watershed, Upper Blue Nile Basin, Ethiopia. *Sustainability* 13 (7), 24. <https://doi.org/10.3390/su13073740>.
- Li, Y., Li, J.L., Chu, J.L., 2022. Research on land-use evolution and ecosystem services value response in mountainous counties based on the SD-PLUS model. *Ecol. Evol.* 12 (10), 18. <https://doi.org/10.1002/ece3.9431>.
- Li, C., Wu, Y.M., Gao, B.P., Zheng, K.J., Wu, Y., Li, C., 2021. Multi-scenario simulation of ecosystem service value for optimization of land use in the Sichuan-Yunnan ecological barrier, China. *Ecol. Indic.* 132, 13. <https://doi.org/10.1016/j.ecolind.2021.108328>.
- Liang, X., Guan, Q.F., Clarke, K.C., Liu, S.S., Wang, B.Y., Yao, Y., 2021. Understanding the drivers of sustainable land expansion using a patch-generating land use simulation (PLUS) model: A case study in Wuhan, China. *Comp. Environ. Urban Syst.* 85, 14. <https://doi.org/10.1016/j.compenvurbusys.2020.101569>.
- Lu, Y.T., Wu, P.H., Ma, X.S., Li, X.H., 2019. Detection and prediction of land use/land cover change using spatiotemporal data fusion and the Cellular Automata-Markov model. *Environ. Monit. Assess.* 191 (2), 19. <https://doi.org/10.1007/s10661-019-7200-2>.
- Reheman, R., Kasimu, A., Duolaiti, X., Wei, B. H., & Zhao, Y. Y. (2023). Research on the change in prediction of water production in urban agglomerations on the northern slopes of the Tianshan Mountains based on the InVEST-PLUS Model. *Water*, 15(4), 19. doi:10.3390/w15040776.
- Shen, J.S., Li, S.C., Liu, L.B., Liang, Z., Wang, Y.Y., Wang, H., Wu, S.Y., 2021. Uncovering the relationships between ecosystem services and social-ecological drivers at different spatial scales in the Beijing-Tianjin-Hebei region. *J. Clean. Prod.* 290, 14. <https://doi.org/10.1016/j.jclepro.2020.125193>.
- Sun, X.Y., Shan, R.F., Liu, F., 2020. Spatio-temporal quantification of patterns, trade-offs and synergies among multiple hydrological ecosystem services in different topographic basins. *J. Clean. Prod.* 268, 12. <https://doi.org/10.1016/j.jclepro.2020.122338>.
- Wang, D., Jing, Y.D., Han, S.M., Cao, M.X., 2022a. Spatio-temporal relationship of land-use carbon emission and ecosystem service value in Mansi Lake Basin based upon a grid square. *Acta Ecol. Sin.* 42 (23), 9604–9614. <https://doi.org/10.5846/stxb202110062753>.
- Wang, X.J., Liu, G.X., Lin, D.R., Lin, Y.B., Lu, Y., Xiang, A.C., Xiao, S.M., 2022c. Water yield service influence by climate and land use change based on InVEST model in the monsoon hilly watershed in South China. *Geomat. Nat. Haz. Risk* 13 (1), 2024–2048. <https://doi.org/10.1080/19475705.2022.2104174>.
- Wang, J., Zhang, J.P., Xiong, N.N., Liang, B.Y., Wang, Z., Cressey, E.L., 2022b. Spatial and temporal variation, simulation and prediction of land use in ecological conservation area of western Beijing. *Remote Sens. (Basel)* 14 (6), 20. <https://doi.org/10.3390/rs14061452>.
- Wang, R.Y., Zhao, J.S., Chen, G.P., Lin, Y.L., Yang, A.R., Cheng, J.Q., 2023. Coupling PLUS-InVEST model for ecosystem service research in Yunnan Province, China. *Sustainability* 15 (1), 19. <https://doi.org/10.3390/su15010271>.
- Wu, C.X., Qiu, D.X., Gao, P., Mu, X.M., Zhao, G.J., 2022. Application of the InVEST model for assessing water yield and its response to precipitation and land use in the Weihe River Basin, China. *J. Arid Land* 14 (4), 426–440. <https://doi.org/10.1007/s40333-022-0013-0>.
- Xie, G.D., Zhang, C.X., Zhang, L.M., Chen, W.H., Li, S.M., 2015. Improvement of ecosystem service valuation method based on unit area value equivalent factor. *J. Nat. Resour.* 30 (8) <https://doi.org/10.11849/rzrzb.2015.08.001>.
- Xu, Q., Yang, R., Zhuang, D.C., Lu, Z.L., 2021. Spatial gradient differences of ecosystem services supply and demand in the Pearl River Delta region. *J. Clean. Prod.* 279, 12. <https://doi.org/10.1016/j.jclepro.2020.123849>.
- Yang, J., Xie, B.P., Zhang, D.G., Tao, W.Q., 2021. Climate and land use change impacts on water yield ecosystem service in the Yellow River Basin, China. *Environ. Earth Sci.* 80 (3), 12. <https://doi.org/10.1007/s12665-020-09277-9>.
- Zhang, L., Cheng, L., Chiew, F., Fu, B.J., 2018. Understanding the impacts of climate and landuse change on water yield. *Curr. Opin. Environ. Sustain.* 33, 167–174. <https://doi.org/10.1016/j.cosust.2018.04.017>.
- Zhang, D., Wang, X., Qu, L., Li, S., Lin, Y., Yao, R., Zhou, X., Li, J., 2020. Land use/cover predictions incorporating ecological security for the Yangtze River Delta region, China. *Ecol. Indic.* 119, 106841.
- Zhang, S.H., Zhong, Q.L., Cheng, D.L., Xu, C.B., Chang, Y.N., Lin, Y.Y., Li, B.Y., 2022. Landscape ecological risk projection based on the PLUS model under the localized shared socioeconomic pathways in the Fujian Delta region. *Ecol. Ind.* 136, 13. <https://doi.org/10.1016/j.ecolind.2022.108642>.
- Zhao, Q.Q., Chen, Y., Gon, K.P., Wells, E., Margeson, K., Sherren, K., 2023. Modelling cultural ecosystem services in agricultural dykelands and tidal wetlands to inform coastal infrastructure decisions: a social media data approach. *Mar. Policy* 150, 10. <https://doi.org/10.1016/j.marpol.2023.105533>.